Journal of ELECTRICAL ENGINEERING, VOL 71(2020), NO4, 237–245

sciendo

PAPERS

Sliding mode controller design for second-order unstable processes with dead-time

Mohammad Atif Siddiqui[1*], Md Nishat Anwar[2], Shahedul Haque Laskar[3]

A new approach is proposed to design the sliding mode (SM) controller for the unstable second-order plus dead-time (SOPDT) processes. The sliding mode control consists of two control laws ie continuous control law and discontinuous control law. The continuous control law parameters have been derived in terms of unstable SOPDT process parameters using the root locus technique. On the other hand, the parameters of discontinuous control law are tuned by optimizing a performance index using a recently developed metaheuristic search algorithm, namely the grasshopper optimization technique. The performance index is framed to achieve a good trade-off between performance and control efforts. Finally, simulations are conducted to validate the effectiveness of the proposed approach over the other existing techniques. It is observed that the proposed approach is able to deliver better disturbance rejection, minimal control efforts and good setpoint tracking.

K e y w o r d s: sliding mode control, unstable process, grasshopper optimization, SOPDT process

1 Introduction

In the most recent period, there is a growing interest in developing robust control methods for systems having modelling errors. Among the existing methods, the sliding mode control (SMC) technique seems a more favourable technique for controlling the plant model with modelling errors [1, 2]. The sliding mode control technique is widely known in the process industry for its property of being robust to modelling errors, external disturbances and parameter variations. These properties make sliding mode control technique quite effective in many practical applications such as in electric drives [3, 4], robotics [5], automotive systems [6], unmanned aerial vehicles [7].

Recently, the use of sliding mode control technique to control chemical processes have gained a lot of attention. Camacho and Smith [8] designed the sliding mode controller based on the stable first order plus dead-time (FOPDT) model for nonlinear chemical processes. The results obtained by Camacho and Smith show large overshoot and long settling time. To overcome the shortcomings of [8], Kaya [9] designed the SM controller by selecting a new sliding surface for the stable processes. Kaya synthesizes the SM controller based on the stable FOPDT model. To solve the issues related to the delay approximation, some researchers [10, 11] adopted Smith predictor (SP) or internal model control (IMC) schemes together with sliding mode control technique to achieve robust performance. Mehta and Kaya [12] used a sliding mode control technique in a complex SP structure, a metaheuristic optimization algorithm and a new power-rate reaching law to control higher-order stable processes. They approximated the higher order model into the stable FOPDT model to synthesize the SM controller. Recently, Herrera *et al* [13] used the FOPDT model-based dynamic sliding mode control procedure in a complex CI&A (compensator of Iinoya and Altpeter) structure to control higher-order processes with time delay and inverse response characteristic. Although complex schemes improved the closed loop performance, but for industrial implementation a simple control structure is much preferred.

The literature cited from [6–13] reveals that many researchers have addressed the design of the SM controller for stable processes. However, very few researchers have carried out research in the design of the SM controller for unstable processes. To control the unstable processes, Rojas *et al* [14] extended the work of Camacho and Cruz [10], both these works, however, uses the FOPDT model to synthesize the SM controller. Later on, the technique of [14] is modified by Sivaramakrishnan *et al* [15] to derive the SM controller parameters to control unstable processes having a dead time to time constant ratio greater than 1. Their method shows little improvement for process uncertainty but not for load disturbance. Mehta and Rojas [16] designed the SM controller for the unstable processes by utilizing the same SP-SMC structure of Mehta and Kaya [12]. They synthesized the SM controller based on the unstable FOPDT model derived by a modified relay experiment. Their method showed merit over the method of Sivaramakrishnan *et al* [15].

In all the schemes reported above, the models utilized to synthesize the sliding mode controller are of a first-order having dead-time. It is to note that for higher-order stable plants, the process can be approximated into

[1] Department of EIE, National Institute of Technology Silchar, India, [2] Department of EE, National Institute of Technology Patna, India, [3] Department of EIE, National Institute of Technology Silchar, India, * Corresponding author: atif.nits@gmail.com

DOI:10.2478/jee-2020–0032, Print (till 2015) ISSN 1335-3632, On-line ISSN 1339-309X

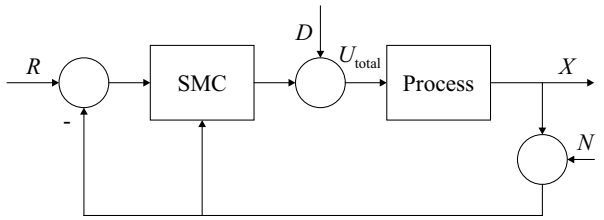

Fig. 1. A simple feedback scheme with SMC

a first-order model having an apparent dead-time and apparent time constant. But, for higher-order unstable plants, a FOPDT model is not adequate to represent its dynamics. The reason being that, apart from unstable dynamic lags, there exist stable time constants in the plant. Thus, utilizing a SOPDT model for unstable-higher order plant would be better because more information regarding the plant dynamics can be represented in SOPDT as compared to FOPDT model. For sliding mode control based on the SOPDT model, there are only a few works reported in the literature [17, 18]. Therefore, proposing a sliding mode technique using an unstable SOPDT model will be valuable for the chemical industry.

Hence, in this paper, a sliding mode controller is designed using the unstable SOPDT model to control second-order unstable processes. A sliding surface having four parameters is introduced to handle the unstable SOPDT processes in a simple structure. The control law parameters are obtained using the set of tuning equations (being developed in terms of SOPDT model parameters), the root locus technique and an advanced metaheuristic search algorithm, namely the grasshopper optimization technique. Simulation examples are presented to demonstrate the efficacy of the proposed SMC method over the recently published approaches.

2 Sliding mode control

The sliding mode control is a robust control scheme that can compensate for inaccuracies in plant modelling. The objective of the sliding mode control is to drag the closed-loop system from its original state to a surface known as a sliding surface. The sliding surface is selected to characterize a desired tracking and stability behaviour. Hence, the initial measure in designing a controller using SMC is to specify the sliding surface $s_s(t)$. Thus, in this work, the sliding surface $s_s(t)$ is

$$s_s(t) = k_1 e(t) + k_2 \int_0^t e(t)\mathrm{d}t + k_3 \frac{\mathrm{d}e(t)}{\mathrm{d}t} + \frac{\mathrm{d}^2 e(t)}{\mathrm{d}t^2}\,. \quad (1)$$

In (1), the terms k_1, k_2 and k_3 are the constant gains and $e(t)$ is the tracking error.

From the control point of view, the aim is to drive and maintain the controlled variable at its reference value. Once the reference value is achieved, (1) indicates that the surface $s_s(t)$ has acquired a constant value meaning that, error and its derivative become zero. So to maintain $s_s(t)$ at a constant value, it is desirable to make its derivative equal to zero and this can be mathematically represented as

$$\frac{\mathrm{d}s_s(t)}{\mathrm{d}t} = \frac{\mathrm{d}^3 e(t)}{\mathrm{d}t^3} + k_2 e(t) + k_3 \frac{\mathrm{d}^2 e(t)}{\mathrm{d}t^2} + k_1 \frac{\mathrm{d}e(t)}{\mathrm{d}t} = 0\,. \quad (2)$$

After selecting the sliding surface, the sliding mode control law is to be developed that satisfy the conditions $s_s(t) = 0$ and its time derivative $s_s'(t) = 0$. The sliding mode control law, U_{tot}, comprises of two components: a continuous component, $U_{cc}(t)$, and a discontinuous component $U_d(t)$

$$U_{\text{tot}}(t) = U_{cc}(t) + U_d(t)\,. \quad (3)$$

The continuous component, $U_{cc}(t)$ is expressed as

$$U_{cc}(t) = f\big(X(t), R(t), e(t)\big). \quad (4)$$

In (4), $f\big(X(t), R(t), e(t)\big)$ is a function of the system output, the reference value and the tracking error.

The discontinuous part, $U_d(t)$, represents the reaching mode which is accountable for directing the system state trajectory towards the sliding surface. Since this part is discontinuous throughout the surface [9, 15, 19], it may result in an undesirable high-frequency oscillation known as chattering. This chattering decreases the accuracy of the controller, causes wear and tear in the actuators and stimulates undesired dynamics. To avoid this chattering, one probable solution [6, 8] is to use

$$U_d(t) = K_D \frac{s_s(t)}{|s_s(t)| + \delta}\,. \quad (5)$$

Here, δ and K_D are the adjusting parameters accountable for minimizing the chattering phenomenon and directing the state trajectory towards the sliding surface, respectively.

3 The proposed sliding mode controller design

In this section, the SM controller for the unstable second-order plus dead-time process (SOPDT) is developed. The design of the continuous component of SMC is discussed first and then the tuning of the discontinuous component of SMC is discussed.

To control the unstable SOPDT process, the control scheme considered is shown in Fig. 1.

In Fig. 1, X is the system output, U_{tot} is the plant input, R is the set-point input, N is the noise input and D is the disturbance input. The unstable SOPDT transfer function is

$$G_p(s) = \frac{x(s)}{u_{\text{tot}}(s)} = \frac{Ke^{-ls}}{(\tau_1 s - 1)(\tau_2 s + 1} \quad (6)$$

where K is the gain, τ_1 and τ_2 are the time constants and l is the dead-time of the plant. In (6), $x(s)$ and $u_{\text{tot}}(s)$ are the Laplace transform of the system output and plant input, respectively. Both $x(s)$ and $u_{\text{tot}}(s)$ are deviation variables. In this work, the dead-time term (e^{-ls}) present in process $G_p(s)$ is ationalized by using the first-order Taylor series approximation that results in the following transfer function

$$G_p(s) = \frac{x(s)}{u_{\text{tot}}(s)} = \frac{K}{\tau_1\tau_2 l s^3 + \big(l(\tau_1-\tau_2)+\tau_1\tau_2\big)s^2 + (\tau_1-\tau_2-l)s - 1} = \frac{K}{c_3 s^3 + c_2 s^2 + c_1 s - c_0}\,. \quad (7)$$

Here, $c_3 = \tau_1\tau_2 l$, $c_2 = l(\tau_1-\tau_2)+\tau_1\tau_2$, $c_1 = \tau_1-\tau_2-l$ and $c_0 = 1$.

From (7), for the controller output U_{tot} is derived as

$$KU_{\text{tot}}(t) = c_3 X'''(t) + c_2 X''(t) + c_1 X'(t) - c_0 X(T) \quad (8)$$

the prime denoting time derivative. Equation (8) is solved for the 3rd order of derivative and is substituted in (2) by considering $e(t) = R(t) - X(t)$, that results in

$$s_s'(t) = \frac{1}{c_3}\big(-KU_{\text{tot}}(t) + c_2 X''(t) + c_1 X'(t) - c_0 X(t)\big) + k_2 e(t) - k_3 X''(t) - k_1 X'(t) = 0\,. \quad (9)$$

For the control law $U_{\text{tot}}(t)$ is derived

$$KU_{\text{tot}}(t) = X''(t)(c_2 - k_3 c_3) + X'(t)(c_1 - k_1 c_3) - c_0 X(t) + k_2 c_3 e(t)\,. \quad (10)$$

It is to note that once the system response reaches the sliding surface, $U_d(t)$ component gets turned off and $U_{\text{tot}}(t)$ corresponds to $U_{cc}(t)$ as

$$KU_{cc}(t) = X''(t)(c_2 - k_3 c_3) + X'(t)(c_1 - k_1 c_3) - c_0 X(t) + k_2 c_3 e(t)\,. \quad (11)$$

Furthermore, the controller's continuous part may be simplified by letting $c_2 - k_3 c_3 = 0$ and $c_1 - c_3 k_1 = 0$ that results in

$$KU_{cc}(t) = -X(t)(c_0 + k_2 c_3) + k_2 c_3 R(t)\,. \quad (12)$$

In SMC, the sliding surface defines the rationale of the closed-loop system. Hence, the condition $U_{cc}(s)G_p(s) = x(s)$ must be satisfied. With this condition, the closed-loop transfer function can be obtained by using (7) and (12) as

$$\frac{x(s)}{r(s)} = \frac{G_p(s)k_2c_3}{K + G_p(s)\,[c_0 + k_2c_3]} = \frac{k_2c_3}{c_3s^3 + c_2s^2 + c_1s + k_2c_3}\,. \quad (13)$$

The last equation is further simplified as

$$\frac{X(s)}{r(s)} = \frac{1}{1 + \left[s^3 + \dfrac{c_2}{c_3}s^2 + \dfrac{c_1}{c_3}s\right]\dfrac{1}{k_2}} = \frac{1}{1 + \widetilde{G}(s)\dfrac{1}{k_2}} \quad (14)$$

and the characteristic equation of the closed-loop system is obtained

$$1 + \widetilde{G}(s)\frac{1}{k_2} = 0\,. \quad (15)$$

The value of k_2 is obtained through the root locus technique. Here, the root locus of $\widetilde{G}(s)$ be plotted in MATLAB environment by using the rlocus command. From the root locus plot, the k_2 value may be selected such that the desired percentage overshoot in the set-point response is obtained. With the selected k_2 value, the design of the continuous control law of the SMC can be completed.

The discontinuous part, $U_d(t)$, as mentioned in (5) have two parameters (K_D and δ). These parameters are accountable for reaching the sliding surface and reducing the chattering problem. It is observed that several researchers have used the metaheuristic algorithm to determine the values of K_D and δ [20]. Nelder and Mead searching algorithm is utilized by [8, 15] to achieve the K_D and δ values. The particle swarm optimization (PSO) technique is utilized by Mehta and Kaya [12] while the cuckoo search (CS) algorithm is adopted by Mehta and Rojas [16] to achieve these values. In this work, a recently developed optimization technique known as grasshopper optimization technique (GOA) is used to tune the K_D and δ values. The reason for using this technique is that it has shown superior performance over many nature-inspired optimization algorithms such as PSO, CS, Genetic algorithm, Ant colony, firefly algorithm [21, 22]. Furthermore, this technique can solve problems with unknown search spaces and delivers superior performance with faster convergence.

$$U_{\text{tot}}(t) = \frac{-X(t)\,[c_0 + k_2c_3] + k_2c_3R(t)}{K} + K_D\frac{s_s(t)}{|s_s(t)| + \delta}\,,$$
$$s_s(t) = \text{sign}(K)\Big(k_1e(t) + k_2\int_0^t e(t)\mathrm{d}t + k_3e'(t) + e''(t)\Big). \quad (16)$$

In (16), the sign(K) is considered to ensure the proper operation of the controller for the particular plant model. It is important to note that the value of sign(K) depends only on the gain of the plant model [19].

4 Grasshopper Optimization Algorithm (GOA)

Grasshoppers are a class of hemimetabolous insects that belong to the Orthoptera (order) and Caelifera (suborder) with dominant rear legs. Grasshopper generally lives a solitary life, but when they become locusts, they form swarms of locusts. This unique behaviour of grasshopper ie foraging and swarming has been mathematically mimicked to propose a grasshopper optimization algorithm (GOA) by Saremi *et al* [21].

Interaction or communication among grasshoppers occurs locally as well as globally. During swarming, they interact globally by exploration and locally by exploitation. The effectiveness of their social communication with respect to exploitation or exploration is possibly defined by a function S (a social force function) as

$$S(r) = -e^{-r} + e^{-r/L} f \tag{17}$$

where, f is the intensity of attraction, r is the random number in $[0, 1]$ and L is the attractive length scale. Any change in f and L parameter will change the social behaviour of the grasshoppers.

In a swarm of G_i (virtual grasshoppers), the population for N search agents can be initialized as

$$\begin{aligned} G_i =& \text{rand}(1, N)(ub_i - lb_i) + lb_i \\ & i = 1, 2, \ldots, \dim \end{aligned} \tag{18}$$

The mathematical representation of i-th position of a search agent along with d-th dimension is given in (19) which mimics the swarming psychology of the grasshopper as

$$X_i^d = C\Big(C\frac{ub_d - lb_d}{2}\sum_{\substack{j\neq i \\ j=1}}^{N} \frac{x_j - x_i}{d_{ij}} S\big(|x_j^d - x_i^d|\big)\Big) + \hat{i}_d \tag{19}$$

$$\left.\begin{matrix} ub_d & \text{is upper bound} \\ lb_d & \text{is lower bound} \end{matrix}\right\} \in d^{th}\text{dimension}$$

x_i is the position of i-th grasshopper, x_j is the position of j-th grasshopper and d-th is the distance between x_i and x_j. C is the decreasing coefficient which balances the exploitation and exploration about the target by minimizing the comfortable distance or comfort zone proportional to the number of iteration. C is estimated as follows

$$C = \frac{C_{\max} - C_{\min}}{\text{Maxitr}}(C_{\max} - l)\,. \tag{20}$$

Here, $C_{\min}$ and $C_{\max}$ are the minimum and maximum values, respectively. The current iteration is indicated by l.

The interaction between grasshoppers with respect to the position of other grasshoppers in a swarm is implemented by the first term in (19) and propensity to progress towards food (target) in d-th dimension is triggered by i_d in (19).

The important features of GOA are

- The position vector in GOA is one for each search agent.
- In the swarm, the position of the search agent is updated by including the current position, global best and the position of each search agent.

The detailed description of GOA is mentioned in [21, 22] and the flowchart of GOA is shown in Fig. 2. In this work, GOA is utilized to optimize the objective function by tuning the discontinuous control law parameters within the specified range (ub and lb). The dimension of the swarm is selected as 2 because the parameters to be tuned by GOA for N search agents are K_D and δ. The parameters for GOA are selected as $C_{max} = 1$, $C_{\min} = 4 \times 10^{-5}$, $f = 0.5$ and $L = 1.5$ and codes are written in .m file of MATLAB. Simulations are performed by utilizing an Intel®core$^{\text{TM}}$ i3-7020U CPU @ 2.3 GHz and 4 GB RAM desktop.

5 Objective function formulation

The objective functions have an important role in resolving optimization problems and choosing the correct error function is the core element of it. Choosing the integral absolute error (IAE) function as an objective function offers an improved performance ie minimizing overshoots and enhancing load disturbance rejection [23]. The IAE function is defined as

$$IAE = \int_0^\infty |R(t) - X(t)|\mathrm{d}t\,. \tag{21}$$

Minimizing the IAE function may not be adequate to claim an optimal controller with minimal control signal variations. Literature reveals that sudden large variation in controller output results in wear and tear of valves which is undesirable. To quantitatively measure the total variation of the controller output, a criterion known as the total variation (TV) is defined by [24] is used here. The TV value of the controller is given as

$$TV = \sum_{i=1}^{\infty} |u_{i+1} - u_i|. \tag{22}$$

In this work, the authors aim to combine the above two quantities to achieve better-closed loop performance along with minimum controller variation. The objective function to be minimized is as

$$J_{\text{tot}} = \sum_{n=1}^{t} \int_0^\infty |R(t_n) - X(t_n)|\mathrm{d}t + \frac{1}{\tau_1}\sum_{n=1}^{t} |u_{n+1} - u_n| \tag{23}$$

where τ_1 is the time constant of the model and t is the total duration of the simulation which is kept greater than the settling time. Here, τ_1 is the constraint imposed on total variation meaning that a small value of τ_1 allows low controller output variation.

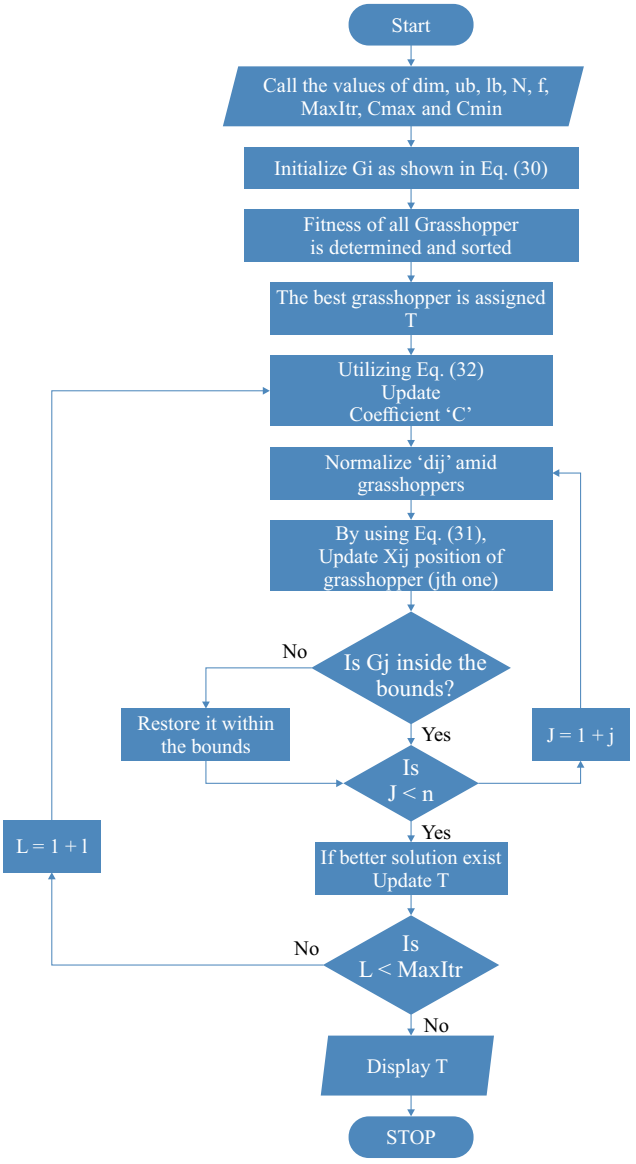

Fig. 2. Flowchart of GOA

6 Simulation results

The performance of the proposed SM controller design method has been compared with the performance of the recently published methods (Mehta and Rojas [16] and Atic and Kaya [25]). The performance has been compared in terms of (i) peak value of the system output ($y_{\max} = \max|Y_1|$), (ii) integral absolute error, (iii) integral square error $\left(ISE = \int_0^\infty (R(t) - X(t)^2 \mathrm{d}t\right)$, (iv) integral time absolute error $\left(ITAE = \int_0^\infty t\,|R(t) - X(t)|\mathrm{d}t\right)$, and (v) total variation (TV). Lesser values of $y_{\max}$, IAE, ISE, $ITAE$ and TV indicate better performance of the closed control system.

6.1 Example 1

In this example, the unstable SOPDT process is taken from the literature Mehta and Rojas [16] as

$$G_p(s) = \frac{e^{-0.5s}}{s^2 + 1.5s - 1}. \tag{24}$$

The method by Mehta and Rojas [16] uses a relay feedback test to approximate this unstable SOPDT process into the FOPDT model as $1.001e^{-1.0587s}/(2s-1)$. The authors have used the approximated FOPDT model and a cuckoo optimization algorithm to design the sliding mode controller in the Smith predictor configuration. Their method has shown better performance compared to earlier mentioned works in the literature. The proposed method uses an unstable SOPDT model and GOA optimization algorithm to obtain the controller parameters as ($k_1 = 3.1$, $k_2 = 1.5$, $k_3 = 4$, $K_D = 32.56$, $\delta = 15$). With these controller settings, both the methods are simulated by applying a setpoint change of magnitude 5 at $t = 0$ s and disturbance change of magnitude -0.1 at $t = 50$ s. The corresponding closed-loop response and the controller response are shown in Fig. 3 and Fig. 4, respectively

Figure 3 and Fig. 4 illustrate that the proposed method delivers significantly improved performance compared to that of the Mehta and Rojas with less controller output variations ($TV = 52.83$). Furthermore, small overshoot with lesser oscillation in setpoint response and prompt disturbance rejection in regulatory response is observed by the proposed method as compared to Mehta

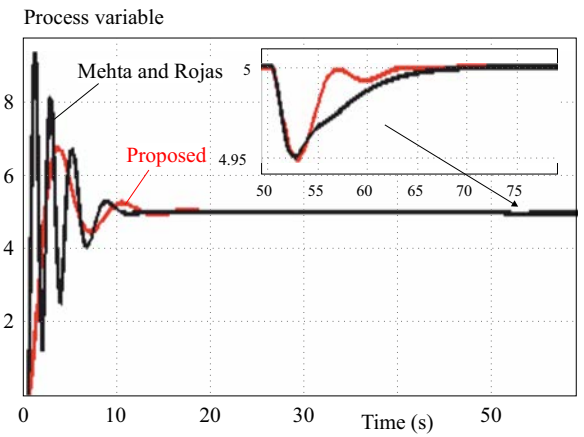

Fig. 3. System response due to input change for $G_p(s) = e^{-0.5s}/(s^2 + 1.5s - 1)$

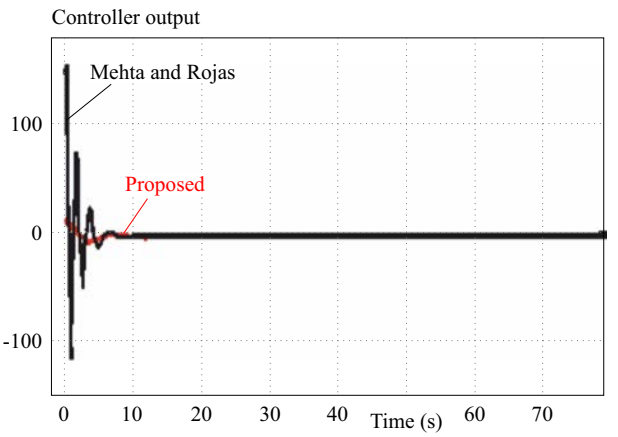

Fig. 4. Controller response due to input change for $G_p(s) = e^{-0.5s}/(s^2 + 1.5s - 1)$

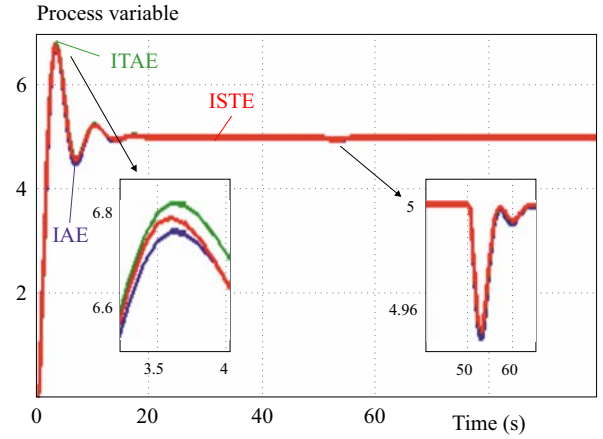

Fig. 5. System response with different objective functions for $G_p(s) = e^{-0.5s}/(s^2 + 1.5s - 1)$

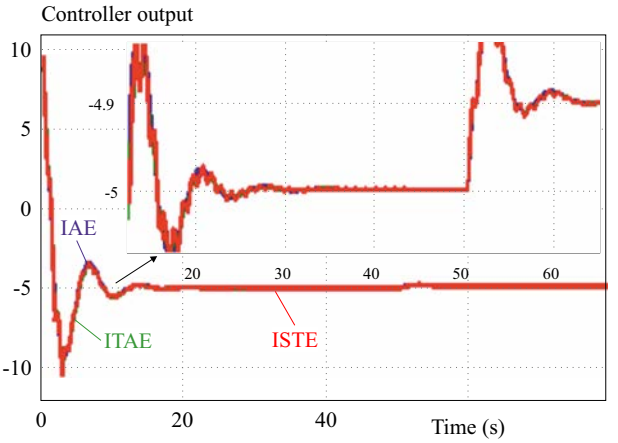

Fig. 6. Controller output with different objective functions for $G_p(s) = e^{-0.5s}/(s^2 + 1.5s - 1)$

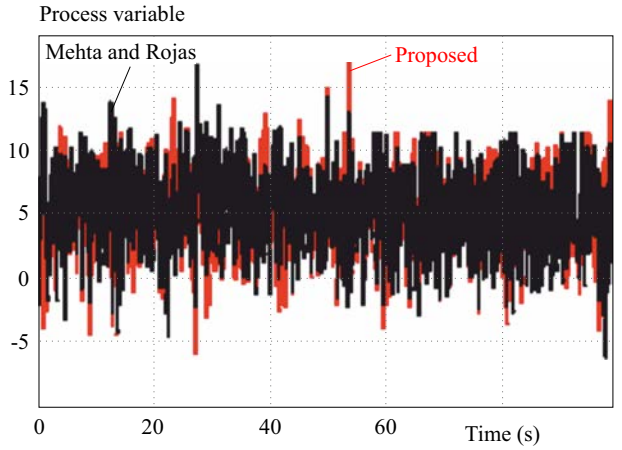

Fig. 7. System response due to noise for $G_p(s) = e^{-0.5s}/(s^2 + 1.5s - 1)$

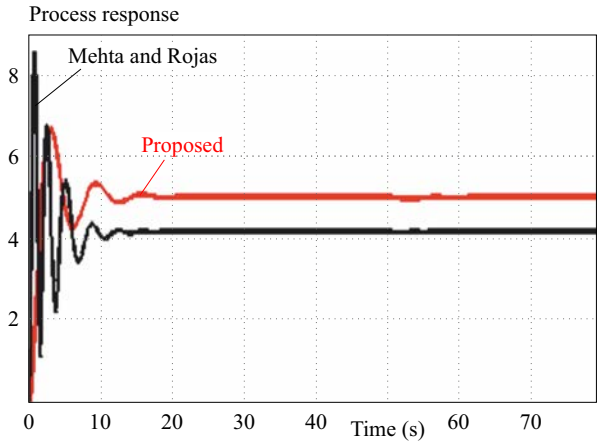

Fig. 8. System response due to perturbation in process parameters for $G_p(s) = e^{-0.5s}/(s^2 + 1.5s - 1)$

and Rojas. The reason for better results by the proposed method in comparison to Mehta and Rojas is due to the use of an unstable SOPDT model instead of an unstable FOPDT model in synthesizing the SMC controller. The performances indices listed in Tab. 1 (Example 1) also indicate better performance of the proposed method as the values of IAE, ISE, $ITAE$, TV and $y_{\max}$ are lower than [16].

The proposed method has been also investigated for different objective functions having $ITAE$ and integral square time error $(ISTE)$ index as given below

$$J_{\mathrm{ITAE,tot}} = \sum_{n=1}^{t} \int_0^{\infty} t|R(t_n) - X(t_n)|\mathrm{d}t + \frac{1}{\tau_1} \sum_{n=1}^{t} |u_{n+1} - u_n|\,, \quad (25)$$

$$J_{\mathrm{ISTE,tot}} = \sum_{n=1}^{t} \int_0^{\infty} \big(tR(t_n) - X(t_n)\big)^2 \mathrm{d}t + \frac{1}{\tau_1} \sum_{n=1}^{t} |u_{n+1} - u_n|\,. \quad (26)$$

Equations (25) and (26) are minimized by GOA and the optimal value of the discontinuous control law parameters (K_D, δ) are obtained as $(16.13, 9.9)$ and $(27.1, 14.03)$, respectively. The system response and controller output for different objective functions are shown in Fig. 5 and Fig. 6. It is observed from Fig. 5 that the overshoot for IAE is minimum whereas the overshoot for $ITAE$ is maximum. The controller output in Fig. 6 indicates that some chattering is observed for the $ISTE$ that may cause wear and tear in the final control elements. From the simulation response, it is observed that the objective function mentioned in (23) is a better choice for obtaining the values of K_D and δ.

In the industrial process, noise may emerge from the process itself, control valves and measurement devices. Therefore, to justify the effectiveness of the present scheme under noisy situations, simulation of the example is conducted by considering the white noise (noise power of 1, seed equal to 0 and sampling time of 0.2 s). The system output under noisy conditions is shown in Fig. 7. For the sake of simplicity, the effect of noise on system output (X) is expressed as $\delta_{X\%} = (\sigma_X/D) \times 100$ [26]. Here, σ_X is the standard deviation of the system out-

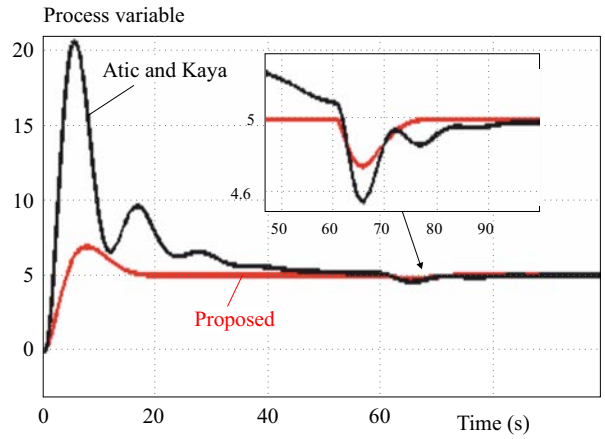

Fig. 9. A composite sample with barely visible impact damage under test: (a) – photograph, (b) – 3D view of the impact image by chromatic confocal optical microscopy

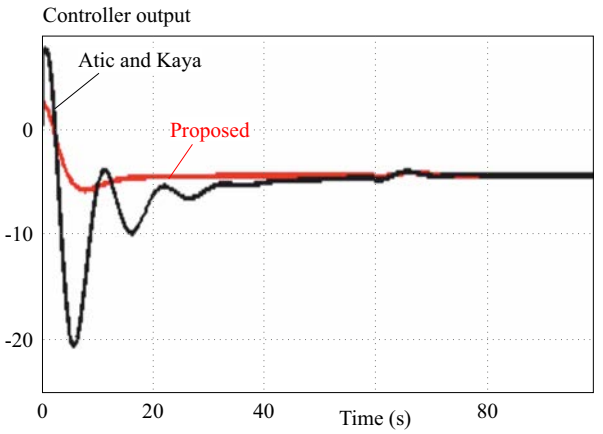

Fig. 10. Frequency responses of the CSRR sensor for impact damage detection

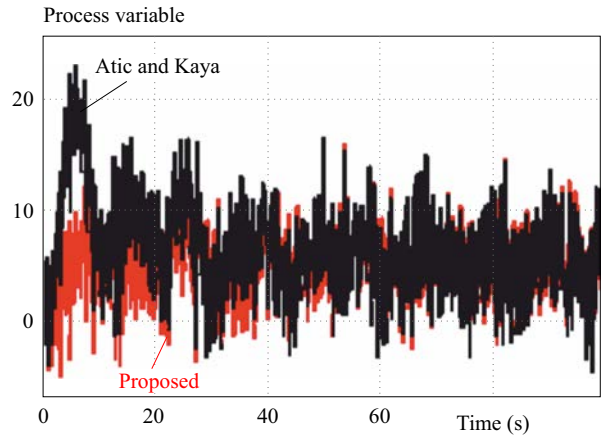

Fig. 11. A composite sample with barely visible impact damage under test: (a) – photograph, (b) – 3D view of the impact image by chromatic confocal optical microscopy

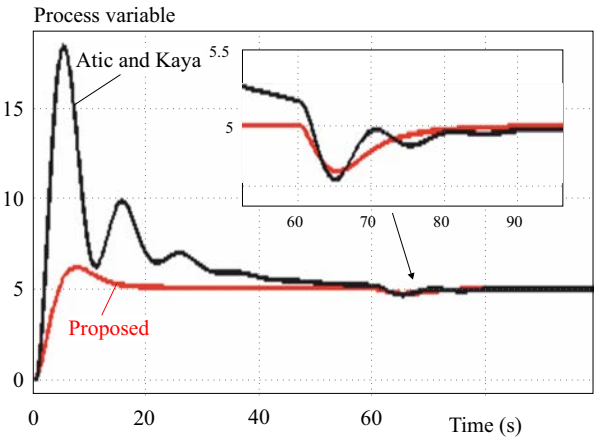

Fig. 12. Frequency responses of the CSRR sensor for impact damage detection

Table 1. Performance indices

Methods	IAE	ISE	$ITAE$	TV	$y_{\max}$		δ_{Y1}
	Complete signal $(R+D_1)$				R	D_1	(%)
Example 1							
Proposed	13.4	36.64	50.2	53.6	6.7	0.044	286
Mehta and Rojas	14.5	39.54	59.4	730	9.38	0.052	289
Example 2							
Proposed	28.6	70.86	280	13.36	6.90	0.25	411
Atic and Kaya	153	1170	2190	78.97	20.6	0.51	512

put under noisy condition and D is the magnitude of the load disturbance which is considered as $D = 1$ at $t = 0$. Calculation of $\delta_{X\%}$ for the proposed method and Mehta and Rojas [16] method are carried out when the system reaches a steady-state. The obtained value of $\delta_{X\%}$ is listed in Tab. 1 (Example 1). From Fig. 7 and Tab. 1, it is observed that the present scheme delivers good performance even in noisy conditions.

A model is generally achieved through some fitting or linearization technique that results in a mismatch between the actual plant and model. Therefore it is critical to analyze the robustness of the control system as a plant model mismatch is inevitable. Hence, the robustness analysis is performed by introducing perturbation of +10 % in gain and time delay of the process. The perturbed system response is shown in Fig. 8.From this, it

can be observed that the design scheme of Mehta and Rojas fails to track the setpoint command while the proposed method allows to track the setpoint command under perturbed conditions. Thus, the overall performance of the proposed method is found better than the method of Mehta and Rojas.

6.2 Example 2

An unstable SOPDT transfer function studied by Atic and Kaya [25] is considered as

$$G_p(s) = \frac{e^{-0.5s}}{(2s-1)(0.5s+1)} \tag{27}$$

Atic and Kaya [25] approximated this process into the FOPDT model ($e^{-0.918s}/(2.69s-1)$) by utilizing a relay feedback test. Based on the FOPDT model, Atic and Kaya obtained the controller settings. The proposed SM controller settings are obtained considering the unstable SOPDT model as $k_1 = 2, k_2 = 0.45$, $k_3 = 3.5$, $K_{\mathrm{D}} = 12.38$, $\delta = 2.69$. With these controller settings, simulations are carried out by applying a step signal of magnitude 5 at $t = 0$ and disturbance signal of magnitude -0.2 at $t = 60$ s. The corresponding closed-loop response and controller output are shown in Fig. 9 and Fig. 10. The performance indices for the setpoint and load disturbance response are listed in Tab. 1, Example 2.

It is observed from Fig. 9 that the present approach delivers reduced overshoot, fast setpoint tracking and enhance load disturbance rejection in comparison with [25]. The performance indices such as IAE, ISE, $ITAE$ and $y_{\max}$ are small and the TV value is also lesser for the present approach (see Tab. 1, Example 2). Also, smooth controller efforts have been observed in Fig. 10 by the proposed method. It is clear from the simulation results that the present approach yields superior closed-loop performance over the method of [25]. The effect of noise is analyzed by applying white noise having noise power of 1, seed equal to 0 and sampling time of 0.1 s. The resulting system output is shown in Fig. 11. For simplicity, the standard deviation of the system output under noisy conditions is calculated after applying a load disturbance change of magnitude 1 at $t = 0$. The obtained $\delta_{X\%}$ is given in Tab. 1, Example 2. From Tab. 1 and Fig. 11, it is observed that the present scheme is less responsive to noise as compared to Atic and Kaya [25] method.

The robustness of the proposed SMC controller is investigated by introducing perturbation of $+10\%$ in K, τ_1 and l simultaneously toward the worst-case model mismatch, *ie* $G_p(s) = 1.1\, e^{(} - 0.55s)/(2.2s-1)/(0.5s+1)$. The perturbed response for both the setpoint change and load disturbance change is given in Fig.12. The presented response indicates that the present scheme has a smooth and fast response. The method of Atic and Kaya [25] shows oscillations with large settling time. The proposed method shows better closed-loop performance, even in perturbed conditions.

7 Conclusions

A simple unstable SOPDT model based sliding mode control scheme is presented for unstable SOPDT processes. The sliding surface is selected and its parameters are obtained using a group of equations that are derived in terms of unstable SOPDT process parameters and applying the root locus technique. The parameters of the reaching mode and the chattering mode are tuned by minimizing IAE performance with TV value using a recently developed metaheuristic algorithm, ie grasshopper optimization algorithm. Through simulation results, it is shown that good set-point tracking, better load disturbance rejection and lower IAE, ISE, $ITAE$, TV and $y_{\max}$ values are obtained by the designed sliding mode controller as compared to some previous methods. The better results of the present scheme are shown with respect to process uncertainty and measurement noise. The proposed method may be extended to higher-order unstable processes.

References

[1] A. Kojima, S. Ishijima, K. Uchida and E. Shimemura, "Robust Stabilization of a System with Delays Control", *IEEE Transactions on Automation Control*, vol. 39, no. 8, pp. 1694–1698, 1994, doi: 10.1109/9.310054.

[2] C. H. Chou and C. C. Cheng, "Design of Adaptive Variable Structure Controllers for Perturbed Time-Varying State Delay Systems", *Journal of Franklin Institute*, vol. 338, no. 1, pp. 35–46, 2001, doi: 10.1016/S0016-0032(00)00070-3.

[3] J. J. Slotine, and S. S. Sastry, "Tracking Control of Non-Linear Systems using Sliding Surfaces with Application to Robot Manipulators", *International Journal of Control*, vol. 38, no. 2, pp. 465–492, 1983, doi: 10.1017/CBO9781107415324.004.

[4] V. I. Utkin, "Sliding Mode Control Design Principles and Applications to Electric Drives", *IEEE Transactions on Industrial Electronics*, vol. 40, no. 1, pp. 23–36, 1993, doi: 10.1109/41.184818.

[5] K. B. Park, and J. J. Lee, "Sliding Mode Controller with Filtered Signal for Robot Manipulators using Virtual Plant/Controller", *Mechatronics*, vol. 7, no. 3, pp. 277–286, 1997, doi: 10.1016/s0957 -4158(97)00001-9.

[6] L. Fu, Ü. Özgüner, and I. Haskara, "Automotive Applications of Sliding Mode Control", *IFAC Proceedings*, vol. 44, no. 1, pp. 1898–1903, 2011, doi: 10.3182/20110828-6-IT-1002.01276.

[7] F. Gavilan, J. Á. Acosta, and R. Vazquez, "Control of the Longitudinal Flight Dynamics of an UAV using Adaptive Backstepping", *IFAC Proceedings Volumes*, vol. 44, no. 1, pp. 1892–1897, 2011, doi: 10.3182/20110828-6-IT-1002.01876.

[8] O. Camacho, and C. A. Smith, "Sliding Mode Control: An Approach to Regulate Nonlinear Chemical Processes", *ISA Transactions*, vol. 39, no. 2, pp. 205–218, 2000, doi: 10.1016/s0019-0578(99)00043-9.

[9] I. Kaya, "Sliding Mode Control of Stable Processes", *Industrial & Engineering Chemistry Research*, vol. 46, no. 2, pp. 571–578, 2007, doi: 10.1021/ie0607806.

[10] O. Camacho, and F. D. la Cruz, "Smith Predictor Based Sliding Mode Controller for Integrating Processes with Elevated Dead-Time", *ISA Transactions*, vol. 43, no. 2, pp. 257–270, 2004, doi: 10.1016/s0019-0578(07)60035-4.

[11] O. Camacho, C. Smith, and W. Moreno, "Development of an Internal Model Sliding Mode Controller", *Industrial & Engineering Chemistry Research*, vol. 42, no. 3, pp. 568–573, 2003, doi: 10.1021/ie010481a.

[12] M. Utkal, and K. Ibrahim, "Smith Predictor with Sliding Mode Control for Processes with Large Dead-Time", *Journal of Electrical Engineering*, vol. 68, no. 6, pp. 463–469, 2017, doi: 10.1515/jee-2017.

[13] M. Herrera, O. Camacho, H. Leiva, and C. Smith, "An Approach of Dynamic Sliding Mode Control for Chemical Processes", *Journal of Process Control*, vol. 85, pp. 112–120, 2020, doi: 10.1016/j.jprocont.2019.11.008.

[14] R. Rojas, O. Camacho, and L. González, "A Sliding Mode Control Proposal for Open-Loop Unstable Processes", *ISA Transactions*, vol. 43, no. 2, pp. 243–255, 2004, doi: 10.1016/s0019- 0578(07)60034-2.

[15] S. Sivaramakrishnan, A. K. Tangirala, and M. Chidambaram, "Sliding Mode Controller for Unstable Systems", *Chemical Biochemical Engineering Quaterly*, vol. 22, no. 1, pp. 41–47, 2008.

[16] U. Mehta, and R. Rojas, "Smith Predictor Based Sliding Mode Control for a Class of Unstable Processes", *Transactions of the Institute of Measurement and Control*, vol. 39, no. 5, pp. 706–714, 2017, doi: 10.1177/0142331215619973.

[17] C. T. Chen, and S. T. Peng, "Design of a Sliding Mode Control System for Chemical Processes", *Journal of Process Control*, vol. 15, no. 5, pp. 515–530, 2005, doi: 10.1016/j.jprocont.2004.11.001.

[18] M. Mihoub, A. S. Nouri, and R. B. Abdennour, "Real-Time Application of Discrete Second Order Sliding Mode Control to a Chemical Reactor", *Control Engineering Practices*, vol. 17, no. 9, pp. 1089–1095, 2009, doi: 10.1016/j.conengprac.2009.04.005.

[19] O. Camacho, R. Rojas, and W. Garca, "Variable Structure Control Applied to Chemical Processes with Inverse Response", *ISA Transactions*, vol. 38, no. 1, pp. 55–72, 1999, doi: 10.1016/S0019-0578(99)00005-1.

[20] A. Ferrara, G. P. Incremona and M.Cucuzzella, "Advanced and Optimization Based Sliding Mode Control: Theory and Applications", *Society for Industrial and Applied Mathematics*, 2019.

[21] S. Saremi, S. Mirjalili, and A. Lewis, "Grasshopper Optimisation Algorithm: Theory and application", *Advances Engineering Software*, vol. 105, pp. 30–47, 2017, doi: 10.1016/j.advengsoft.2017.01.004.

[22] A. K. Barik, and D. C. Das, "Expeditious Frequency Control of Solar Photovoltaic/Biogas/Biodiesel Generator Based Isolated Renewable Microgrid using Grasshopper Optimisation Algorithm", *IET Renewable Power Generation*, vol. 12, no. 14, pp. 1659–1667, 2018, doi: 10.1049/iet-rpg.2018.5196.

[23] M. A. Sahib and B. S. Ahmed, "A New Multiobjective Performance Criterion Used PID Tuning Optimization Algorithms", *Journal of advanced research*, vol. 7, no. 1, pp. 125–134, 2016, doi: 10.1016/j.jare.2015.03.004.

[24] S. Skogestad, "Simple Analytic Rules for Model Reduction and PID Controller Tuning", *Journal of Process Control*, vol. 13, no. 4, pp. 291–309, 2003, doi: 10.4173/mic.2004.2.2.

[25] S. Atic and I. Kaya, "PID Controller Design Based on Generalized Stability Boundary Locus to Control Unstable Processes with Dead-Time", *26th Mediterranean Conference on Control and Automation*, pp. 436–441, 2018, doi: 10.1109/MED.2018.8442568.

[26] M. Č. Bošković, T. B. Šekara, and M. R. Rapaić, "Novel Tuning Rules for PIDC and PID Load Frequency Controllers Considering Robustness and Sensitivity to Measurement Noise", *International Journal of Electrical Power & Energy Systems*, vol. 114, pp. 105416–105430, 2020.

Received 16 June 2020

Mohammad Atif Siddiqui received a bachelor's and master's degree in Electronics and Communication Engineering from Integral University, Lucknow, India. He is currently pursuing a PhD degree from NIT, Silchar in Electronics & Instrumentation Engineering Department since 2015. His research interest includes Sliding mode control, Cascade control, PID controller and PIDA controller.

Md Nishat Anwar received his bachelor's and master's degree in Electrical Engineering from AMU, Aligarh, India. He obtained his PhD from IIT (ISM), Dhanbad, India in 2015. He has teaching experience of 5 years and currently working as an Assistant Professor in the Department of Electrical Engineering, NIT Patna, India. His research interests include industrial control and automation, PID controller, sliding mode control.

Shahedul Haque Laskar was born in Nitainagar (Hailakandi), Assam (India) in 1962. He attended Irfan Ali Memorial H.S. School, Nitainagar and Public H.S. School, Hailakandi. He did Pre-university from Cotton College, Guwahati (1977-79) and engineering courses from graduate up to research from Z.H. College of Engg & Tech, AMU, Aligarh. He joined teaching as a lecturer in Electrical Engineering Department, REC (presently NIT), Silchar in 1991 and now working as Associate Professor and head in the Electronics & Instrumentation Engineering Department, NIT Silchar. In addition to life members of ISTE (India), he is in the elite group of elected IEEE Senior Members and a member of the IEEE Instrumentation & Measurement Society. He has been working in the domain of instrumentation including measurements and sensing.